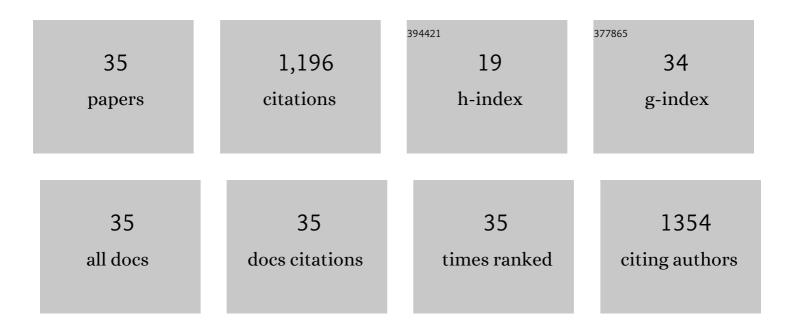
Liu Shu-Sheng

List of Publications by Year in descending order

Source: https://exaly.com/author-pdf/6086739/publications.pdf Version: 2024-02-01



#	Article	IF	CITATIONS
1	The destabilization mechanism and de/re-hydrogenation kinetics of MgH2–LiAlH4 hydrogen storage system. Journal of Power Sources, 2008, 185, 1514-1518.	7.8	101
2	Facile fabrication of long α-Fe2O3, α-Fe and γ-Fe2O3 hollow fibers using sol–gel combined co-electrospinning technology. Journal of Colloid and Interface Science, 2007, 308, 265-270.	9.4	99
3	Transcriptome analysis and comparison reveal divergence between two invasive whitefly cryptic species. BMC Genomics, 2011, 12, 458.	2.8	99
4	Superior hydrogen storage properties of MgH2–10Âwt.% TiC composite. Energy, 2010, 35, 3417-3421.	8.8	92
5	Effect of ball milling time on the hydrogen storage properties of TiF3-doped LiAlH4. International Journal of Hydrogen Energy, 2009, 34, 8079-8085.	7.1	87
6	Enhanced Hydrogen Storage Performance of LiBH ₄ â^'SiO ₂ â^'TiF ₃ Composite. Journal of Physical Chemistry C, 2008, 112, 4005-4010.	3.1	67
7	Why solid oxide cells can be reversibly operated in solid oxide electrolysis cell and fuel cell modes?. Physical Chemistry Chemical Physics, 2015, 17, 31308-31315.	2.8	63
8	Improved hydrogen desorption properties of ammonia borane by Ni-modified metal-organic frameworks. International Journal of Hydrogen Energy, 2011, 36, 6698-6704.	7.1	61
9	Significantly improved dehydrogenation of LiAlH4 destabilized by K2TiF6. International Journal of Hydrogen Energy, 2012, 37, 3261-3267.	7.1	57
10	The Dehydrogenation Reactions and Kinetics of 2LiBH4â^'Al Composite. Journal of Physical Chemistry C, 2009, 113, 18424-18430.	3.1	47
11	Hydrogen storage properties of destabilized MgH2–Li3AlH6 system. International Journal of Hydrogen Energy, 2010, 35, 8122-8129.	7.1	42
12	Improved reversible hydrogen storage of LiAlH4 by nano-sized TiH2. International Journal of Hydrogen Energy, 2013, 38, 2770-2777.	7.1	41
13	NiCo nanoalloy encapsulated in graphene layers for improving hydrogen storage properties of LiAlH4. Scientific Reports, 2016, 6, 27429.	3.3	37
14	Metals (Ni, Fe)-Incorporated Titanate Nanotubes Induced Destabilization of LiBH ₄ . Journal of Physical Chemistry C, 2011, 115, 9780-9786.	3.1	35
15	The dehydrogenation performance and reaction mechanisms of Li3AlH6 with TiF3 additive. International Journal of Hydrogen Energy, 2010, 35, 4554-4561.	7.1	31
16	Dehydrogenation process of AlH3 observed by TEM. Journal of Alloys and Compounds, 2013, 580, S163-S166.	5.5	28
17	Thermodynamics study of hydrogen storage materials. Journal of Chemical Thermodynamics, 2012, 46, 86-93.	2.0	24
18	Sulfur poisoning behavior of La1-xSrxCo1-yFeyO3-δthin films with different compositions. Journal of Alloys and Compounds, 2018, 748, 608-619.	5.5	21

LIU SHU-SHENG

#	Article	IF	CITATIONS
19	Improved dehydrogenation of MgH2–Li3AlH6 mixture with TiF3 addition. International Journal of Hydrogen Energy, 2011, 36, 11785-11793.	7.1	19
20	Time-Dependence of Surface Composition, Transport Properties Degradation, and Thermodynamic Consideration of La0.6Sr0.4Co0.2Fe0.8O3-δunder Chromium Poisoning. Journal of the Electrochemical Society, 2018, 165, F1206-F1216.	2.9	19
21	Determination of Factors Governing Surface Composition and Degradation of La _{0.6} Sr _{0.4} Co _{0.2} Fe _{0.8} O ₃₋ <i>_î</i> Electrode under Sulfur-Contained Air. Journal of the Electrochemical Society, 2019, 166, F414-F422.	2.9	19
22	Evolution of cathode-interlayer interfaces and its effect on long-term degradation. Journal of Power Sources, 2020, 453, 227894.	7.8	18
23	Atomic structure observations and reaction dynamics simulations on triple phase boundaries in solid-oxide fuel cells. Communications Chemistry, 2019, 2, .	4.5	16
24	Microstructure evolution of NiO–YSZ cermet during sintering. Solid State Ionics, 2014, 262, 460-464.	2.7	13
25	Observation of the Ni/YSZ Interface in a Conventional SOFC. Journal of the Electrochemical Society, 2015, 162, F750-F754.	2.9	13
26	A Fundamental Study of Boron Deposition and Poisoning of La _{0.8} Sr _{0.2} MnO ₃ Cathode of Solid Oxide Fuel Cells under Accelerated Conditions. Journal of the Electrochemical Society, 2015, 162, F1282-F1291.	2.9	13
27	Influence of electrolyte substrates on the Sr-segregation and SrSO4 formation in La0.6Sr0.4Co0.2Fe0.8O3_δthin films. MRS Communications, 2019, 9, 236-244.	1.8	12
28	Progress in improving thermodynamics and kinetics of new hydrogen storage materials. Frontiers of Physics, 2011, 6, 151-161.	5.0	6
29	Image contrast enhancement of Ni/YSZ anode during the sliceâ€andâ€view process in FIB‧EM. Journal of Microscopy, 2016, 261, 326-332.	1.8	5
30	Microstructure Observation of Ni/YSZ Boundary by TEM and STEM. ECS Transactions, 2013, 57, 1401-1405.	0.5	3
31	Boundary Observation and Contrast Tuning of Ni/YSZ Anode by TEM and FIB-SEM. ECS Transactions, 2015, 68, 1275-1279.	0.5	3
32	Microscopic Studies on the Secondary Phases in LSCF after Cr Poisoning. ECS Transactions, 2019, 91, 1257-1262.	0.5	2
33	Dependence of the Electrochemical Performance of Ni/YSZ Anode on Water Vapor Partial Pressure. ECS Transactions, 2019, 91, 1973-1978.	0.5	2
34	Multi-Scale, Multi-Physics Approach for Solid Oxide Fuel Cell Anode Reaction. ECS Transactions, 2017, 78, 2835-2844.	0.5	1
35	B22-P-06Ni/YSZ Interface in A Conventional Solid Oxide Fuel Cell. Microscopy (Oxford, England), 2015, 64, i105.2-i105.	1.5	0